THE JOURNAL OF PHYSICAL CHEMISTRY B

Article

pubs.acs.org/JPCB

Li^+–Oligoglyme Association in the Presence of Ionic Liquid Studied by Molecular Dynamics and Explicit or Implicit Solvent Model

Andrzej Eilmes* and Piotr Kubisiak

Faculty of Chemistry, Jagiellonian University, Ingardena 3, 30-060 Kraków, Poland

Supporting Information

ABSTRACT: Molecular dynamics simulations have been applied to study properties of ternary oligoglyme/ionic liquid/lithium salt electrolytes. Different types of lithium coordination and phase behavior have been observed depending on the liquid/salt anion: from full phase separation and Li^+ coordination exclusively to anions in systems with BF_4^- to rather homogeneous systems and prevailing Li^+–hexaglyme coordination for FSI^- or $B(CN)_4^-$ anion. Observed structural properties have been successfully correlated to the binding energies of Li^+–glyme complexes in solution calculated within an explicit solvent model. Conversely, an implicit solvent approach has failed to predict differences between electrolytes based on different ionic liquids.

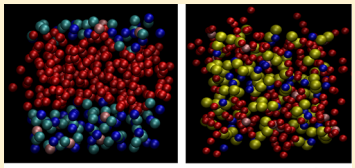

1. INTRODUCTION

Solid polymer electrolytes attract considerable attention owing to their applications in fuel cells, secondary lithium batteries, and electrochemical devices. Several attractive features of these electrolytes, including easy preparation, good mechanical properties, and safety of use, stimulate continuing interest in their research and development.[1−4] Electrolytes of this type consist of inorganic salt dissolved in a polymer matrix, e.g., poly(ethylene oxide) (PEO).[5] Lithium cations are therefore solvated by oxygen atoms from polymer backbone and relatively strong Li^+–polymer interactions hinder mobility of cations.[6] Another disadvantage of PEO-based electrolytes is a high degree of crystallinity.[7] These factors result in the rather low ionic conductivity of solid polymer electrolytes at room temperatures.[2,3,8]

A common approach to improve conductivity of PEO electrolytes is the addition of compounds of low molecular weight acting as plasticizers, reducing crystallinity, increasing segmental motion of polymer backbone, and enhancing ionic transport.[3,4,8,9] Commonly used plasticizers are poly(ethylene glycol) or organic carbonates, such as propylene carbonate or ethylene carbonate.[3,4] However, they are volatile and flammable compounds, increasing potential hazards; therefore, their use raises safety concerns.

On the other hand, organic salts with low melting points, known as room-temperature ionic liquids, possess several advantages: low volatility, nonflammability, and thermal and electrochemical stability.[4,10,11] Ionic liquids (ILs) are therefore prospective solvents to replace molecular liquids in electrochemical devices. Addition of an ionic liquid lowers viscosity of the system and enhances segmental mobility of PEO chains, thus increasing mobility of ions.[12]

Several experimental studies have been conducted on ternary polymer/salt/ionic liquid electrolytes (mainly based on lithium salts, but including also several systems with sodium or magnesium ions) and their physicochemical, electrochemical, and spectral properties.[13−27] The possibility of using different salts and ionic liquids (sharing common anion or with different anions) in different ratios allows for vast variety of such systems. An alternative way to prepare systems with IL and oligoether components is to use functionalized ionic liquids with oligoether chains incorporated into cations of the IL.[28−30]

Experimental studies are assisted by computational research aimed at modeling of electrolyte systems toward better understanding and, ultimately, prediction of their properties. Structural and transport properties of complex electrolytes are typically studied by classical molecular dynamics (MD) simulations. Such an approach has been applied also to PEO-based electrolytes plasticized by ionic liquids.[12,31−34] MD computations are an invaluable tool in research on polymer electrolytes and ionic liquids; however, they need long simulation time and very often require development or modification of force field (FF) parametrization.

Properties of an electrolyte depend on the strength of interactions between ions and molecules, and such data are available from quantum-chemical (QC) calculations. Because of computational costs, their routine use is limited to studying structure and interactions in relatively small systems. Nevertheless, they provide valuable data and numerous computational studies have been performed on glyme/salt complexes[35−39] as well as on ionic liquids;[40−44] of necessity, only selected representative works are mentioned here. Typically, QC methods are used to calculate properties in vacuum; therefore, their results correspond to the gas phase rather than to condensed matter, such as electrolytes. In particular, the dielectric medium considerably affects strength of interactions involving charged species.

Received: April 8, 2015
Revised: July 30, 2015
Published: August 5, 2015

DOI: 10.1021/acs.jpcb.5b05705
J. Phys. Chem. B 2015, 119, 11708−11720

Computationally cheap methods of accounting for the solvent effects in QC calculations are the implicit solvent models, e.g. COSMO[45] or polarizable continuum model (PCM).[46] Several attempts have been made to apply continuous solvent models in theoretical investigations of interactions in PEO-based electrolytes or similar systems.[47−50] The problem of solvent effects naturally arises also in QC computations of interaction strength for ternary PEO/salt/IL mixtures.

In this work we want to examine different ways of accounting for the solvent effect of ionic liquid or PEO matrix for binding energies of Li^+−oligoglyme complexes. An explicit solvent model will be employed, and its predictions will be compared to those of the standard PCM approach. Results of solvent models will be used to rationalize structures of the systems obtained from MD simulations. In this way we will obtain information on the applicability of cost-effective implicit solvent models to the prediction of properties of mixed PEO/IL solutions.

2. METHODOLOGY

We studied oligoglyme/lithium salt/ionic liquid electrolytes. Short oligoether molecules (from diglyme to hexaglyme) were used as models of the PEO part of experimentally investigated systems. Ionic liquids investigated here were based on 1-ethyl-3-methylimidazolium (EMIM) cation and five anions: tetracyanoborate ($B(CN)_4^-$), tetrafluoroborate (BF_4^-), hexafluorophosphate (PF_6^-), bis(fluorosulfonylimide) (FSI^-), and bis(trifluoromethane)sulfonimide ($TFSI^-$). Lithium salts shared the anions of ILs.

Polarizable force field was used in molecular mechanics and molecular dynamics calculations. The part describing ionic liquids and lithium salts (Li^+ and EMIM cations and all anions), based on the APPLE&P (atomistic polarizable potential for liquids, electrolytes & polymers) force field,[51] was adopted from our recent work on ionic liquids.[52] Bonded parameters for oligoglymes were taken also from the APPLE&P parametrization. The form of the nonbonded parameters in APPLE&P (Buckingham-type van der Waals parameters and electrostatic interactions of lone pairs at oxygen atoms) was unsuitable for direct use in our MD software, and for this part of force-field we used parameters (employing Lennard-Jones potential and partial charges located on atoms) from an earlier work on PEO-based electrolytes[53] with small modification (decrease of polarizability of C atom) to improve reproduction of binding energies. Performance of this parametrization was checked by optimizing geometries of Li^+−oligoglyme complexes with increasing coordination number (CN) in MP2/aug-cc-pVDZ calculations and in the force-field and by comparing structural parameters and binding energies obtained from these two approaches; results are presented in Supporting Information.

Model electrolyte systems were composed of hexaglyme (HG) and lithium salt (O_{HG}:Li ratio equaled approximately 20:1) and contained varying amounts (0, 10, 20, or 50 weight-%) of ionic liquid with the same anion as the salt. Detailed numbers of molecules and ions in each system may be found in the section presenting results of MD simulations. Initial random structures of electrolytes were prepared with the Packmol package.[54] MD simulations were conducted using Tinker 5.1 molecular modeling software.[55] Each system was simulated in the *NPT* ensemble at P = 1 atm and at two temperatures, 400 and 323 K (except for electrolytes with PF_6^- anions for which the lower temperature was raised to 353 K because of higher melting point of EMIM-PF_6 IL). In all cases the Berendsen thermostat[56] was used. Default Tinker value of 0.1 ps was used as the coupling time for the temperature bath. The Beeman algorithm[57] with time step of 1 fs was used to integrate the equations of motion. Electrostatic interactions were treated via Ewald summation.[58] Induced dipoles were calculated in an iterative scheme assuming mutual interactions between polarizable atoms to achieve self-convergence; the Thole scheme of short-range polarization damping[59] was applied. Individual frames from MD simulations were saved for further analysis in 5 ps intervals, and the simulations lasted 15−25 ns.

We applied a sequential MD/QC procedure to obtain binding energies in explicit solvents. First, we performed additional MD simulations for each solute frozen in its MP2/aug-cc-pVDZ geometry solvated in a box of 60 hexaglyme molecules or 100 pairs of ions of an ionic liquid. Investigated solutes were oligoglyme molecules from diglyme to hexaglyme (in all-*trans* geometries) and their complexes with Li^+ cation with coordination numbers ranging from CN = 1 to CN = 7. Structures of all complexes are presented in Supporting Information; for CN = 6, there are two structures: one with hexaglyme and the other with two diglyme molecules labeled CN6 and CN6′, respectively. Note that the structures of Li−glyme complexes were frozen at the vacuum QC geometry; therefore, Li−O distances for extreme (low or high) coordination numbers do not represent well the distances for real systems. We used these structures mainly to analyze the solvent effect on a larger set of data. On the other hand, complexes with CN = 4 or CN = 5 are representative examples of dominant Li^+ coordination according to experimental data and unfrozen MD simulations discussed in section 4. In addition to complexes, Li^+ and individual anions solvated in HG were simulated. Simulations of solvated solutes in frozen geometry were performed in *NVT* ensemble at T = 298 K (353 K for systems in EMIM-PF_6). The size of the periodic simulation box was set to reproduce the density of neat hexaglyme or ionic liquid. Initial relaxation of the systems with frozen solute geometry lasted about 4−5 ns. After that time approximately 400 frames (2 ns of trajectory) were collected for further analysis.

In the next step, from the recorded MD trajectories we extracted geometries of solutes solvated in the increasing number of HG molecules or IL ion pairs. The Trajectory Sculptor tool[60] was applied to extract from each frame the central solute and the nearest solvent molecules or ions. Obtained structures were used in subsequent energy calculations (QC- or FF-based).

Quantum chemical MP2/aug-cc-pVDZ calculations for individual solutes (molecules, ions, or complexes) in vacuum or in the implicit solvent (modeled via polarizable continuum model) were performed using Gaussian 09, rev. D.01.[61] In density functional theory (DFT) calculations for solutes solvated in aggregates of HG molecules or IL ions, we employed TeraChem, v1.5[62] to take advantage of hardware acceleration on Nvidia M2090 and Nvidia K20 Graphics Processing Units. In our previous study,[52] we encountered convergence problems when functionals without long-range corrections were used for aggregates of IL ions; accordingly, TeraChem computations were performed at the CAM-B3LYP/6-31+G* level to avoid such complications.

DOI: 10.1021/acs.jpcb.5b05705
J. Phys. Chem. B 2015, 119, 11708−11720

3. INTERACTION AND BINDING ENERGIES

3.1. Explicit Solvent Model. Using the structures obtained from MD simulations with frozen solutes, we calculated interaction and binding energies. In Figure 1 we show a schematic representation of the computational procedure used to visualize solute/solvent structures and corresponding energy terms.

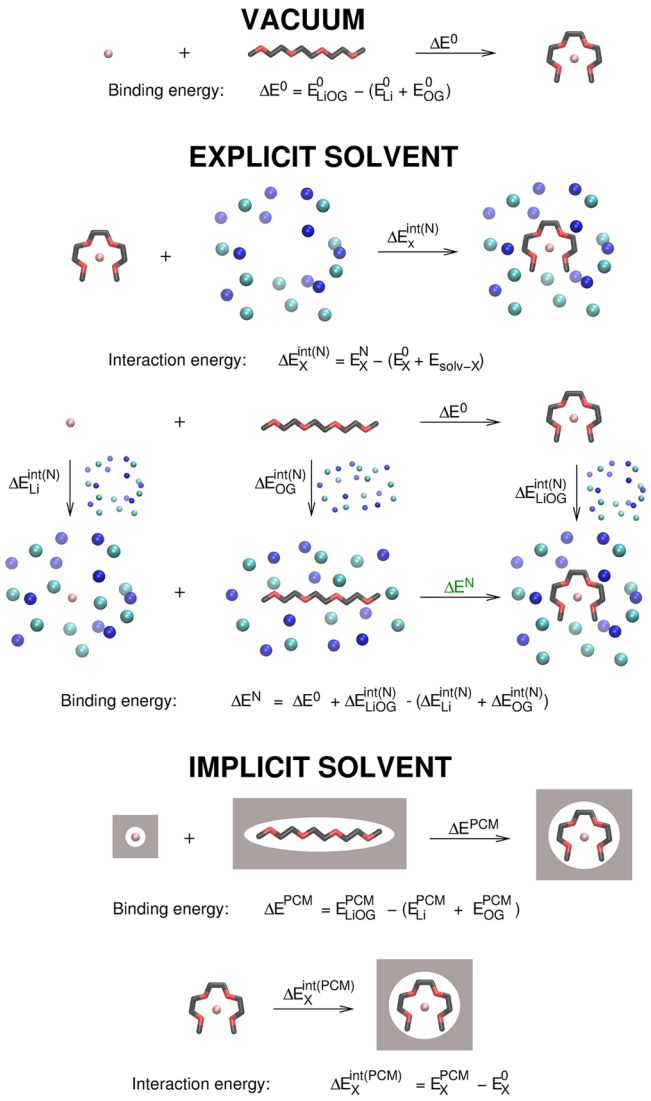

Figure 1. Schematic presentation of computational procedure used to calculate interaction and binding energies in vacuum; explicit and implicit solvent based on structures obtained from MD simulations. A simplified representation of solute and solvent molecules and ions is used for clarity.

Strength of the solvation effect may be estimated from the energy of interaction between solute and the solvent. Interaction energies, $\Delta E_X^{int(N)}$, between the solute X and N hexaglyme molecules or N ion pairs of ionic liquid were calculated as

$$\Delta E_X^{int(N)} = E_X^N - (E_X^0 + E_{solv-X}) \quad (1)$$

N or 0 specify the amount of the solvent (that is, E_X^0 stands for the energy calculated in vacuum) and E_{solv-X} is the energy of N solvent molecules or ion pairs in the geometry of the system [X + solvent]. The latter value was obtained for each system from an additional energy calculation for the solvent "droplet" with the solute X removed. The advantages of this definition are that energy fluctuations caused by different arrangements of solvent molecules and ions partially cancel between E_X^N and E_{solv-X} and the scatter of calculated $\Delta E_X^{int(N)}$ is significantly reduced.

Binding energies of Li^+−oligoglyme complexes in vacuum were calculated as

$$\Delta E^0 = E^0_{LiOG} - (E^0_{Li} + E^0_{OG}) \quad (2)$$

where E_X^0 is the energy of species X (X = complex Li−OG, Li^+, or oligoglyme molecule in its optimal geometry) calculated in vacuum. On the basis of a thermodynamic cycle, we used vacuum values of binding energies and the energies of the interaction with the solvent to obtain binding energies in solution (in N solvent molecules or ion pairs):

$$\Delta E^N = \Delta E^0 + \Delta E^{int(N)}_{LiOG} - (\Delta E^{int(N)}_{Li} + \Delta E^{int(N)}_{OG}) \quad (3)$$

The largest N values used in calculations were 39 molecules of hexaglyme and 60 ion pairs of IL. To make the computations tractable, we applied molecular mechanics with the force field used in MD to calculate interactions and binding energies. Results were averaged over about 400 structures (last 2 ns of the MD trajectory).

In Figure 2 we display selected examples of how the interaction energy changes with increasing amount of the solvent (ionic liquid or hexaglyme) solvating the solute: hexaglyme molecule, Li^+ cation, or Li^+−oligoglyme complexes with CN = 1 or CN = 6. In hexaglyme, all $\Delta E_X^{int(N)}$ values decrease monotonically with N. The strongest is the interaction with small lithium cation, and the weakest is with neutral HG molecule. In the complex with oligoglyme, the charge of Li^+ is screened; therefore, interactions of complexes with the solvent are weaker than in the case of bare Li^+. In the complex with CN = 6, screening is quite effective, so that $\Delta E_X^{int(N)}$ is only 5 kcal/mol lower than the value for electrically neutral hexaglyme.

In ionic liquids the picture is more complicated. Interaction energy calculated for the HG molecule depends on N in a similar way as in hexaglyme solution, and the values in ILs are only 5−10 kcal/mol lower than those in molecular solvent. On the other hand, $\Delta E_X^{int(N)}$ for Li^+ ion or its complex with CN = 1 are significantly more negative. Moreover, when N increases, values of interaction energy oscillate, as is readily seen in Figure 2a,b. This effect results from strong electrostatic interactions between charged solute and the ions of ionic liquid, giving rise to structure of solvation shells with alternating sign of interaction with the solute. The first minimum in $\Delta E_X^{int(N)}$ is caused by the shell of IL anions closest to the central cation. Net charge of the next shell is positive, resulting in the maximum of the interaction energy. Interactions of charged solute with ionic liquid are therefore of long-range nature, and the net effect arises from the sum of contributions from consecutive solvation shells. As seen in Figure 2, oscillations of interaction energy persist even up to 60 pairs of IL ions. Charge of Li^+ ion in the complex with CN = 6 is screened by the ligand molecule, and the solvent-structuring effect is less pronounced, though still noticeable. No oscillations are observed in hexaglyme solutions because solvent molecules are electrically neutral; therefore, different solvation shells are less structured and do not give alternating contributions to the total interaction energy.

DOI: 10.1021/acs.jpcb.5b05705
J. Phys. Chem. B 2015, 119, 11708−11720

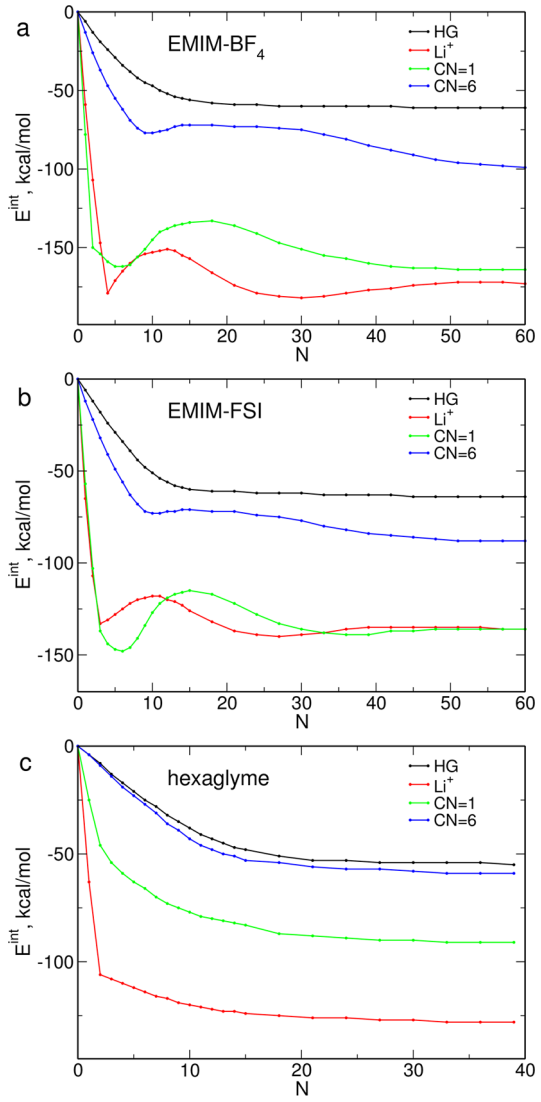

Figure 2. Solute−liquid $\Delta E_X^{\mathrm{int}(N)}$ interaction energies calculated in explicit solvent for increasing number, N, of solvent molecules or ions.

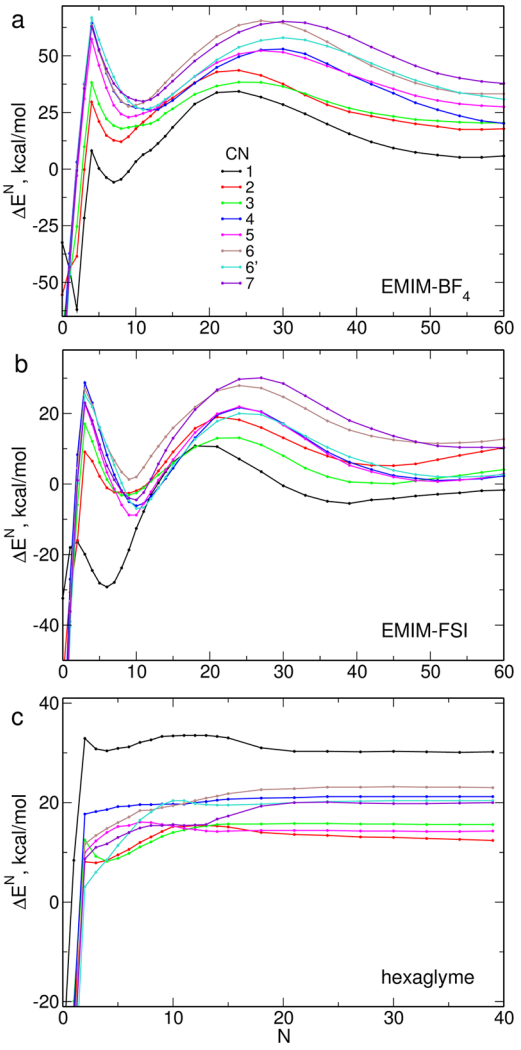

Figure 3. Binding energies of Li^+−oligoglyme complexes calculated in explicit solvent for increasing number, N, of solvent molecules or ions.

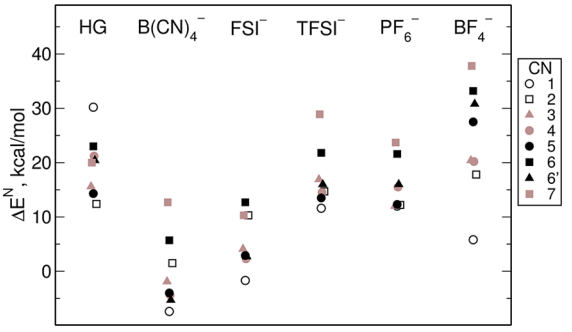

Figure 4. Binding energies of Li^+−oligoglyme complexes obtained in hexaglyme or in EMIM IL (with specified anion) for largest systems with explicit solvent.

This behavior is reflected in binding energies of Li^+−oligoglyme complexes in solution calculated according to eq 3. In ionic liquids, ΔE^N oscillates when the number of solvent ion pairs increases, as seen in Figure 3a,b, and the effect is non-negligible even for the largest droplet sizes used in calculations. Conversely, in hexaglyme, binding energies become approximately constant above 20 solvating HG molecules as a result of weaker solute−solvent interactions and less structured solvation shells.

To compare binding energies in different solvents, we plotted in Figure 4 ΔE^N values obtained for largest N used in calculations (i.e., 39 for hexaglyme and 60 for ILs). Most values are positive with the exception of some complexes in EMIM-$B(CN)_4$ and the complex CN = 1 in EMIM-FSI. We will discuss the sign later; at this point we compare relative stabilization energies. Binding energies of Li^+ complexes with oligoglymes depend on the ionic liquid used as a solvent and increase in the order EMIM-$B(CN)_4$ < EMIM-FSI < EMIM-TFSI ≈ EMIM-PF_6 < EMIM-BF_4. Increase of binding energies is related to the energies of interaction with the solvent, especially to the interaction energy of Li^+ (Table 1). Lithium cation in EMIM-BF_4 is much better stabilized than in EMIM-$B(CN)_4$ or in EMIM-FSI, and more negative value of $\Delta E_{\mathrm{Li}}^{\mathrm{int}(N)}$ increases the binding energy ΔE^N obtained from eq 3. Binding energies in hexaglyme are similar to the values obtained in EMIM-TFSI or EMIM-PF_6. Although in this case Li^+ interaction with the solvent is the weakest, simultaneously also the stabilization of the Li^+−oligoglyme complex in the solvent is weaker than in ionic liquids, resulting in moderate binding energies.

DOI: 10.1021/acs.jpcb.5b05705
J. Phys. Chem. B 2015, 119, 11708−11720

Table 1. Interaction Energies with the Solvent (kcal/mol) Calculated within the PCM Approach and in Explicit Solvents for Li^+, Diglyme (DG), Hexaglyme (HG), and Selected Li^+−Oligoglyme Complexes[a]

solvent	Li^+	DG	HG	CN1	CN3	CN5	CN6	CN7
PCM, def., ε = 5	−98.5	−3.1	−6.3	−64.9	−42.5	−31.7	−30.3	−29.0
PCM, def., ε = 15	−115.0	−4.0	−8.0	−78.7	−50.7	−37.0	−35.4	−33.8
PCM, def., ε = 80	−121.6	−4.4	−8.9	−84.7	−54.2	−39.1	−37.5	−35.8
PCM, UAKS, ε = 5	−98.5	−10.4	−25.1	−76.5	−53.1	−49.2	−48.6	−48.9
PCM, UAKS, ε = 15	−115.0	−13.5	−32.6	−92.9	−63.5	−58.9	−58.4	−59.2
PCM, UAKS, ε = 80	−121.6	−15.0	−36.1	−100.1	−67.9	−63.1	−62.8	−63.9
PCM, SMD, ε = 5	−73.0	−4.7	−11.8	−55.1	−46.8	−41.2	−40.2	−40.8
PCM, SMD, ε = 15	−85.1	−6.8	−15.1	−66.4	−51.1	−48.4	−47.1	−47.9
PCM, SMD, ε = 80	−90.1	−7.8	−18.4	−71.4	−54.2	−51.3	−50.0	−51.0
explicit HG	−128.5	−26.0	−55.1	−91.9	−67.9	−60.1	−59.9	−67.8
explicit EMIM-$B(CN)_4$	−128.2	−28.8	−66.0	−132.0	−87.8	−82.3	−84.0	−85.8
explicit EMIM-FSI	−136.9	−30.4	−64.3	−136.6	−92.1	−86.9	−88.6	−95.2
explicit EMIM-TFSI	−144.7	−28.2	−58.4	−128.9	−85.0	−79.2	−80.9	−78.5
explicit EMIM-PF_6	−155.8	−27.2	−52.4	−138.7	−100.0	−87.7	−88.7	−88.8
explicit EMIM-BF_4	−173.0	−29.5	−61.6	−164.4	−111.1	−96.3	−99.3	−101.1

[a]Labeling of complexes as in Supporting Information.

One may note that in ILs usually the complex with CN = 1 has the lowest binding energy. This is caused by its stabilizing interaction with the ionic liquid, which is similar to the effect observed for bare Li^+ ion. For larger coordination numbers, this interaction is reduced because of more effective screening of cation charge. Conversely, in hexaglyme the CN = 1 complex is the least stable, and in this case it is a result of weak binding in vacuum (less negative ΔE^0).

Up to now we have discussed interaction and binding energies obtained using the force field. We were therefore able to calculate energies up to tens of solvent molecules or ion pairs in the aggregate and easily average data over several hundreds of structures. Nevertheless, it is interesting to get some information about the values resulting from quantum-chemical calculations. For selected systems (Li^+, diglyme, and Li^+−diglyme complex with CN = 1) we performed quantum-chemical CAM-B3LYP/6-31+G* calculations in explicit EMIM-TFSI solvent. Even though GPU acceleration was employed, computational time necessary to complete the calculations forced us to limit both the system sizes (to maximum 15 pairs of IL ions) and the number of structures used in averaging (to about 20).

Comparison between FF and quantum-chemical data is presented in Figure 5. Though there are differences in interaction energies obtained from the two approaches, quantum-chemical data follow the trend shown by FF results. For diglyme and the complex with Li^+ ion, inclusion of Grimme's D3 empirical correction for dispersion[63] apparently improves agreement between interaction energies calculated from QC and FF methods. Moreover, values of binding energy shown in Figure 5b do not depend on the use of empirical dispersion because corrections to interaction energies cancel in ΔE^N. Results of force field calculations agree well with the QC data, especially for systems with larger numbers of explicit IL ion pairs. We concluded therefore that fast method of force-field-based energy computations captures well the physics of interactions in the studied systems as confirmed by test QC calculations.

3.2. Continuous Solvent Approach. Predictions of explicit solvent model may be compared to the values obtained from the polarizable continuum model.[46] We used PCM with default Gaussian 09 parameters applied to construct the molecular cavity (universal force field atomic radii and scaled van der Waals surface). Two other sets of atomic radii were also tested: united atom Kohn−Sham radii (UAKS) and the radii derived from the SMD solvation model.[64] Interaction energies of the solute with the solvent were calculated as a difference between energies obtained in the PCM solvent and in vacuum. Binding energies in implicit solvent were obtained by replacing vacuum values of energy in eq 2 by the values computed within the PCM (cf. Figure 1). We used three values of static dielectric constant: ε = 5 corresponding to oligoglyme solutions; ε = 15, close to values typical for EMIM ionic liquids; and ε = 80 as a limiting case highly polar solvent.

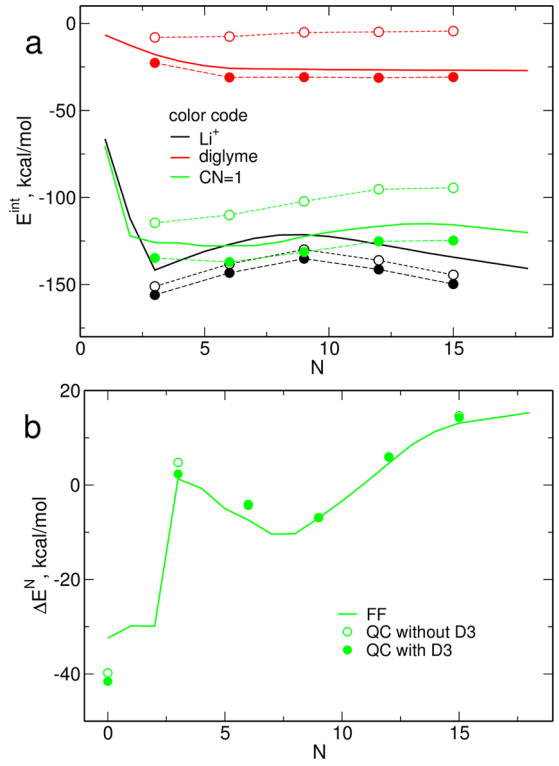

Figure 5. Comparison of solute−solvent interaction energies (a) and binding energies (b) obtained from force field (solid lines) and CAM-B3LYP/6-31+G* (symbols and broken lines) calculations.

DOI: 10.1021/acs.jpcb.5b05705
J. Phys. Chem. B 2015, 119, 11708−11720

Table 2. Binding Energies (kcal/mol) Calculated within the PCM Approach and in Explicit Solvents for Li^+−Oligoglyme Complexes[a]

solvent	CN1	CN2	CN3	CN4	CN5	CN6	CN6′	CN7
vacuum	−37.2	−64.5	−80.0	−96.8	−110.6	−119.4	−130.2	−128.2
PCM, def., ε = 5	−0.5	−13.9	−20.9	−29.9	−39.1	−45.6	−55.4	−52.3
PCM, def., ε = 15	3.0	−6.5	−11.8	−18.8	−26.6	−32.8	−42.2	−39.0
PCM, def., ε = 80	4.0	−3.7	−8.2	−14.3	−21.5	−27.6	−36.8	−33.5
PCM, UAKS, ε = 5	−4.8	−16.5	−24.2	−34.0	−43.5	−48.0	−57.0	−53.4
PCM, UAKS, ε = 15	−1.6	−8.9	−15.0	−23.1	−31.5	−35.1	−43.9	−39.8
PCM, UAKS, ε = 80	−0.7	−5.8	−11.3	−18.6	−26.6	−29.7	−38.5	−34.2
PCM, SMD, ε = 5	−14.6	−33.6	−45.9	−58.7	−70.6	−77.0	−88.0	−84.2
PCM, SMD, ε = 15	−11.7	−27.8	−39.1	−51.0	−62.3	−67.8	−78.8	−74.6
PCM, SMD, ε = 80	−10.7	−25.5	−26.3	−47.7	−58.7	−63.9	−75.0	−70.0
explicit HG	30.2	12.4	15.6	21.2	14.3	23.0	20.4	20.0
explicit EMIM-$B(CN)_4$	−7.4	1.5	−1.9	−4.4	−4.0	5.7	−5.3	12.7
explicit EMIM-FSI	−1.7	10.3	4.1	2.3	2.9	12.7	2.7	10.3
explicit EMIM-TFSI	11.6	14.7	16.9	14.5	13.5	21.8	16.0	28.9
explicit EMIM-PF_6	12.0	12.2	12.0	15.5	12.3	21.6	16.0	23.7
explicit EMIM-BF_4	5.8	17.8	20.4	20.2	27.5	33.2	30.8	37.8

[a]Labeling of complexes as in Supporting Information.

Interaction energies are summarized in Table 1, including also the values calculated in explicit solvents for largest system sizes. As expected, strongest stabilization in the solvent is encountered by Li^+ ion and by complexes with low coordination numbers because these solutes produce the strongest electric field. Interactions of highly coordinated complexes in which the cation is hidden inside the complex are weaker, and the smallest effect is observed for electrically neutral oligoglyme molecules. These observations are valid both in implicit and in explicit solvent; however, interaction energies obtained from the explicit model are in most cases more negative (stronger stabilization). Increasing dielectric constant of the solvent increases polarization of the medium and thus decreases interaction energies. Values obtained for UAKS radii are lower than those resulting from default parametrization. Effect of SMD-derived radii depends on the solute. For Li^+ and low coordination numbers, SMD calculations yield energies higher than those of the two other parametrizations; for oligoglymes and complexes with large CNs, SMD results are between those obtained using default and UAKS radii.

It may be easily noted that even the PCM-UAKS interaction energies in the medium with ε = 80 are almost always less negative than the values obtained in explicit hexaglyme (i.e., in the solvent with low dielectric constant). For ε = 5 (corresponding to hexaglyme) stabilization in implicit solvent is significantly too low. In explicit ionic liquids, interaction energies decrease; therefore, difference with implicit solvent models (with ε = 15) becomes even larger than for HG. Continuous solvent models seriously underestimate solute−solvent interaction strength (even when an unreasonably large dielectric constant equal 80 is used); the difference is the largest for Li cation and complexes with small CNs. From the three parametrizations of atomic radii tested in our calculations, the UAKS model yielded the smallest difference with explicit solvent data.

Interaction energies of oligoglymes with ionic liquid do not depend much on the IL. Conversely, for Li^+, ΔE^{int} decreases from EMIM-$B(CN)_4$ to EMIM-BF_4 by about 45 kcal/mol; quite large changes are observed also for some complexes. These differences between ionic liquids could not be obtained from typical continuous models such as PCM because their predictions depend mainly on the value of the dielectric constant of the liquid, and this parameter is similar for all ILs studied in this work.

Binding energies obtained from different models are summarized in Table 2. Implicit solvent model reduces stabilization of the complex compared to the energy in vacuum. This reduction becomes larger with increasing dielectric permittivity of the medium. The lowest binding energies were obtained from the SMD-based radii, and this result may be attributed to reduced interaction energy of Li^+, as shown above. All variants of the PCM approach yield the same sequence of binding energies as calculated in vacuum−stabilization increases from small to large coordination numbers. Almost all values (except for weakly bound complexes in highly polar medium) are negative because the main effect captured by the model is the electrostatic screening rescaling vacuum values of binding energies.

This is not the case in explicit solvent. The large interaction energy of free Li^+ with the solvent destabilizes the complex according to eq 3, and the binding energies are positive. The net effect of binding is the balance between stabilization energy in vacuum and interaction energies of individual ions or molecules with the solvent; therefore, there is no such simple sequence of changes of ΔE with increasing CN as in implicit models. As stated before, a large interaction energy of the CN = 1 complex with ionic liquid causes this complex in IL solutions to have the lowest binding energy. As in the case of interaction energies, continuous solvent model can account for the difference between hexaglyme and ionic liquids because they differ in dielectric constant but cannot differentiate between ILs studied in this work.

The most striking difference between implicit and explicit solvent models is the different sign of the binding energies. Complexation energies obtained from continuous solvent models are usually negative, and this does not reflect well the physical reality because complexes break up in real solutions. On the other hand, explicit solvent changes the sign of calculated binding energies as shown in several studies[47,50,52] and seen in Table 2, suggesting dissociation of complexes in the solvent. Therefore, rather than drawing conclusions about the

DOI: 10.1021/acs.jpcb.5b05705
J. Phys. Chem. B 2015, 119, 11708−11720

stability of a single complex from either model, predictions about *relative* stabilities of different complexes can be made based on stabilization energies calculated within the same approach.

4. RESULTS OF MOLECULAR DYNAMICS SIMULATIONS

MD simulations of ternary electrolytes were performed for hexaglyme/lithium salt solutions with increasing content of each of five ILs investigated here. Densities of simulated systems (averaged over last 2 ns of the trajectory) are displayed in Table 3. Length of MD trajectories is insufficient to reliably calculate transport properties with reasonable errorbars, and this was not the goal of the work; nevertheless, we present some rough estimates of diffusion coefficients and conductivities in Supporting Information. In this section we will analyze obtained structures of electrolytes and try to relate them to binding energies calculated in the preceding section.

Table 3. Details of Composition of Electrolytes (Number of Hexaglyme Molecules, Li^+–Anion Pairs of the Salt, EMIM–Anion Pairs of IL) and Simulated Densities

					density [g/cm^3]	
IL anion	IL %	n(HG)	n(salt)	n(IL)	323 K[a]	400 K
BF_4^-	0	54	19	0	1.11	1.03
	10	52	18	10	1.12	1.04
	20	46	16	20	1.13	1.06
	50	32	11	55	1.18	1.10
PF_6^-	0	54	19	0	1.13	1.08
	10	50	18	8	1.15	1.11
	20	48	17	17	1.18	1.13
	50	32	11	45	1.25	1.21
$TFSI^-$	0	54	19	0	1.20	1.11
	10	51	18	6	1.22	1.14
	20	46	16	12	1.24	1.16
	50	33	12	35	1.33	1.25
FSI^-	0	54	19	0	1.17	1.09
	10	49	17	7	1.18	1.11
	20	49	17	16	1.21	1.13
	50	33	12	43	1.27	1.20
$B(CN)_4^-$	0	54	19	0	1.09	1.02
	10	52	18	9	1.08	1.02
	20	45	16	17	1.08	1.02
	50	30	11	47	1.07	1.00

[a]353 K for EMIM-PF_6

In the course of simulations we observed substantial reorganization of some systems, eventually leading to separation of hexaglyme and IL phases. The easiest way to spot the differences in the structures of HG/salt/IL solutions is to examine the systems containing 50% of IL simulated in the higher temperature (400 K). Selected snapshots are presented in Figure 6. For clarity, only selected atoms are displayed, including Li^+ cation, oxygen atoms from the hexaglyme molecule, and one of nitrogen atoms from $EMIM^+$ cation.

Phase separation apparently occurred in the system with EMIM-BF_4; ionic liquid and hexaglyme form two different phases, and it may be easily seen that Li^+ ions reside in the IL phase. Separation of the IL is visible also in the system with EMIM-PF_6, although in this case the interface between the two phases is less clearly pronounced. On the other hand,

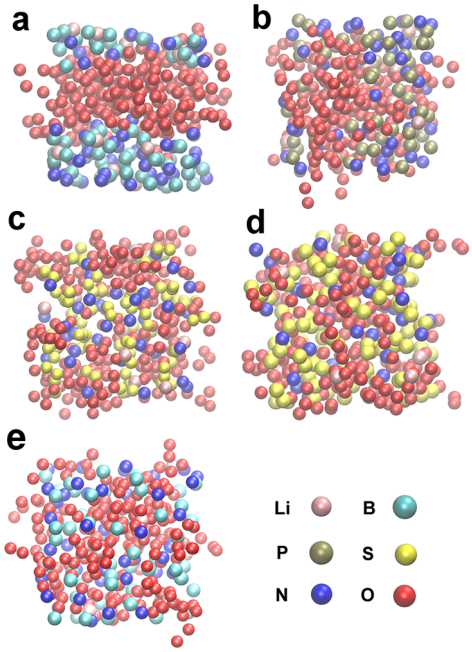

Figure 6. Structures of hexaglyme/salt/ionic liquid electrolytes with different anions: BF_4^- (a), PF_6^- (b), $TFSI^-$ (c), FSI^- (d), and $B(CN)_4^-$ (e).

hexaglyme and ions are much better mixed in solutions with $TFSI^-$, FSI^-, or $B(CN)_4^-$ ions. In these systems, domains of HG or IL are small and both systems seem rather homogeneous. In EMIM-FSI and EMIM-$B(CN)_4$, Li^+ cations are complexed mainly by O atoms from hexaglyme molecules, as seen in Figure 6d,e. Similar are the pictures for other IL concentrations and lower temperature, with an obvious difference that for low amount of ionic liquid domains of separated IL phase are smaller. Separated PEO domains solvated in IL are common structures observed in experiments on PEO/salt/IL electrolytes; for examples, see photographs in refs 21 and 23.

To get more insight into coordination of lithium cation, we examined the radial distribution functions (RDFs) and integrated RDFs giving distance-dependent coordination numbers of Li^+. Plots obtained for 400 K are displayed in Figure 7 for Li–$O_{(HG)}$ pairs and Li–X, where X is the coordinating atom from the IL anion, i.e., F atom in the case of BF_4^- and PF_6^- and O atom from FSI^- or $TFSI^-$ (plots for EMIM-$B(CN)_4$ and for lower temperature can be found in Supporting Information). In all cases (Li–O and Li–F distributions) a sharp peak appears in the RDF at about 2 Å; for clarity, in Figure 7 we displayed RDFs only for systems without IL. Integrated RDFs, yielding running coordination numbers, clearly show different types of Li^+ coordination depending on the anion used in the electrolyte. In the systems with BF_4^-, lithium cation is coordinated mainly to F atoms. In TFSI and PF_6-based electrolytes, Li^+ is approximately equally coordinated to hexaglyme and to salt/IL anions, whereas in the systems with FSI^- and $B(CN)_4^-$, coordination to hexaglyme oxygen atoms dominates.

Average numbers of coordinating atoms found up to the distance of 3 Å (oxygen atoms from hexaglyme, FSI^-, or $TFSI^-$ and nitrogen atoms from $B(CN)_4^-$) or 2.5 Å (fluorine atoms from BF_4^- or PF_6^- anions) from the central Li^+ ion are collected in Table 4; the last 2 ns of trajectories were used for

DOI: 10.1021/acs.jpcb.5b05705
J. Phys. Chem. B 2015, 119, 11708–11720

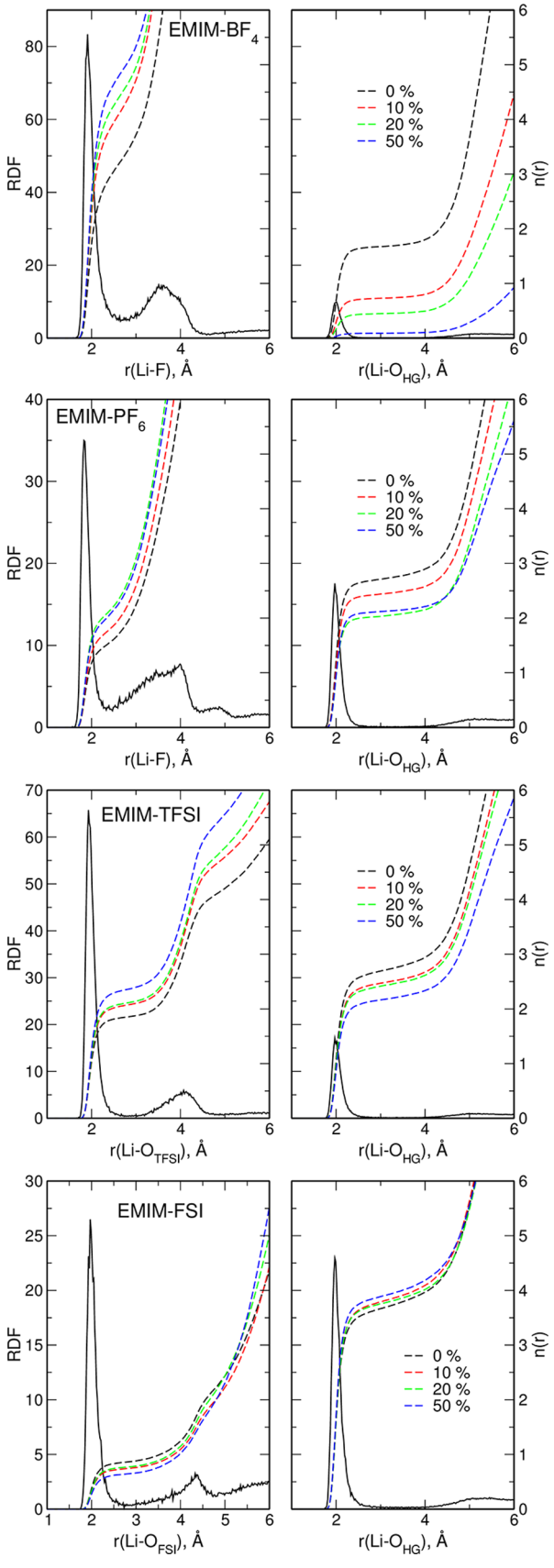

Figure 7. Li–X radial distribution functions and distance-dependent coordination numbers, $n(r)$, obtained in MD simulations of electrolytes with different ionic liquids at 400 K.

averaging. In the systems with $TFSI^-$ and PF_6^- ions, Li^+ cation is coordinated to about 2–3 oxygen atoms from hexaglyme molecule and to 1.5–2.2 fluorine atoms from PF_6^- or 1.6–2.4 oxygen atoms from $TFSI^-$ anion. Coordination to hexaglyme decreases with increasing concentration of IL or increasing temperature; simultaneously, coordination to the anion increases. Increased Li^+ coordination to $TFSI^-$ anions observed when the amount of TFSI-based IL in the system increases is consistent with Raman spectroscopy experiments[24] and the conclusions of ref 16. The same trend, but more pronounced, is observed in systems with EMIM-BF_4. Even in systems without ionic liquid, coordination to BF_4^- anions is preferred. For large IL concentration there is practically no coordination to hexaglyme molecules, and the cation interacts with almost 5 fluorine atoms in concordance with qualitative conclusions based on Figure 6a. At the other end there are systems with EMIM-FSI and EMIM-$B(CN)_4$. In this case, lithium cation is coordinated mainly by hexaglyme (about 4–5 oxygen atoms), the number of coordinating oxygen atoms from FSI^- anions is less than 1, and coordination to $B(CN)_4^-$ is negligible. There is practically no correlation of CNs with the amount of IL, and the effect of increasing temperature is a small decrease of Li–$O_{(HG)}$ coordination.

Experimental information available on Li^+ coordination in PEO/oligoglymes or in ionic liquids comprises mainly structural and spectroscopic data on Li^+–oligoglyme solvates[65−74] and the Raman spectroscopy studies on Li^+–anion interactions in ionic liquids.[75−81] Such measurements on ternary oligoglyme/salt/IL electrolytes are less common;[21,22,24,29] therefore, there are not much experimental data available for direct comparison with our simulations. Nevertheless, Li^+–oligoglyme solvates and lithium salt solutions in ionic liquids are two extreme cases, and we may try to compare such systems to our electrolytes with 0% and 50% amount of an IL, respectively.

Coordination of Li^+ with anions was experimentally investigated via Raman spectroscopy; interactions with the cation lead to appearance of new vibrational bands in the spectrum of the anion, with energy shifted from the position for free anion. Analysis of experimental data and results of molecular dynamics simulations led to the conclusion that in solutions with FSI^- or $TFSI^-$ anions there is a significant amount of monodentate Li^+–(T)FSI^- coordination.[76,79,82,83] Likewise, simulations for pyrrolidinium-based liquid predicted almost exclusively monodentate coordination of Li^+ by BF_4^- anions.[83] In our simulations the number of oxygen atoms from FSI^- or $TFSI^-$ anion in the coordination shell of Li^+ remains low, implying monodentate coordination. On the other hand, in the system with 50% EMIM-BF_4, the Li^+ cation is surrounded in average by 4.6 fluorine atoms. The number of BF_4^- anions up to 4 Å distance is about 3.5; therefore, the ratio of monodentate to bidentate coordinating anions is approximately 2:1 and is smaller than that observed in ref 83. Similar estimate shows that in the electrolyte with 50% EMIM-PF_6, more that 80% of PF_6^- ions are engaged in monodentate coordination. High-energy X-ray diffraction data[81] suggest that the Li^+–O_{anion} distance in Li^+–FSI^- aggregates is larger than in Li^+–$TFSI^-$ (1.94 and 1.86 Å, respectively). This increase is also observed in our data: maximum of Li–O_{anion} RDF shifts from 1.93 Å for $TFSI^-$ ions to 1.99 Å in systems with FSI^-.

Oligoglyme molecules and lithium salts form solvate ionic liquids in which strong interactions between oligoglyme ligands and the cation lead to formation of complex ions. Such systems

DOI: 10.1021/acs.jpcb.5b05705
J. Phys. Chem. B 2015, 119, 11708–11720

Table 4. Average Numbers of Li^+-Coordinating Atoms Found up to 2.5 Å (Li−F Coordination) or 3 Å (Li−O or Li−N Coordination) Distance from the Lithium Cation

		T = 323 K[a]				T = 400 K			
anion	atom	0%	10%	20%	50%	0%	10%	20%	50%
BF_4^-	$O_{(HG)}$	2.1	1.3	1.0	0.1	1.7	0.7	0.4	0.1
	F	2.8	3.5	3.8	4.6	3.1	4.0	4.3	4.7
PF_6^-	$O_{(HG)}$	2.9	2.6	2.6	2.1	2.7	2.4	2.0	2.1
	F	1.5	1.7	1.7	2.2	1.6	1.9	2.2	2.2
$TFSI^-$	$O_{(HG)}$	3.2	2.7	2.9	3.2	2.7	2.5	2.4	2.2
	$O_{(TFSI)}$	1.6	2.1	1.9	1.6	1.9	2.1	2.1	2.4
FSI^-	$O_{(HG)}$	4.2	4.3	4.4	4.0	3.7	3.8	3.8	3.9
	$O_{(FSI)}$	0.5	0.5	0.4	0.7	0.9	0.8	0.8	0.7
$B(CN)_4^-$	$O_{(HG)}$	4.8	4.8	4.8	4.7	4.5	4.5	4.5	4.5
	N	0.0	0.1	0.0	0.1	0.1	0.1	0.1	0.1

[a]353 K for EMIM-PF_6.

may be viewed as concentrated solutions of lithium salts. Many such solvates have been obtained in crystalline form, and X-ray structural data are available for these structures.[65−68,70,72,73] According to these data, the preferred coordination number of Li^+ to oxygen atoms is 4 or 5.[65,66,68] When there is no direct cation interaction with the anion, these coordination sites are occupied by glyme oxygens. Accordingly, maximum ionicity was observed in glyme/TFSI solvate ionic liquids[69] for O:Li ratio between 4 and 5, suggesting that the first solvation shell of Li^+ contains 4−5 oxygen atoms. Typically, Li^+−O_{glyme} distances in crystalline structures are close to 2 Å.[66,67,70,73] Molecular dynamics simulations for lithium salt solutions in oligoglymes or poly(ethylene oxide) also predict the maximum of Li−O RDF at about 2 Å.[84−86] Therefore, average coordination numbers of 4−4.8 found in our simulations for Li^+ interacting with hexaglyme and the position of the first peak in RDF agree well with experimentally determined features. Likewise, the maximum of Li−F RDF at 1.91 Å obtained in our systems with EMIM-BF_4 is consistent with Li−F distances in the range of 1.83−1.95 found for crystalline solvates with $LiBF_4$.[72] At this point we should note that although local coordination of Li^+ interacting with oligoglyme seems fairly well reproduced, the hexaglyme chain is too short to exhibit some features of long poly(ethylene oxide) chains, in particular, helical conformations adopted by polymer backbone[86] (although an incomplete helical turn may be spotted in complexes CN = 6 or CN = 7). However, we had to use short oligomers in order to make energy calculations in explicit solvent tractable. This difference in PEO chain structure is likely to affect the mechanism of ion transport, which is not discussed in this work focused on energetics.

Solvates of lithium salts exhibit different degrees of ion association ranging from solvent-separated ion pairs, through contact ion pairs, to aggregate solvates. Strength of ionic association correlates with the type of salt anion.[68] According to ref 68, the degree of ionic association increases in the order $TSFI^-$ < PF_6^- < BF_4^-. Li^+ coordination to the salt/IL anion increases in the same order observed in our MD simulations.

Interactions with Li^+ change the geometry of the anion (bond length and angles) and therefore induce changes in vibrational spectra. Raman spectroscopy is therefore widely used to assess the degree of ion association in PEO/oligoglyme electrolytes, and the analysis is supported by theoretical calculations.[72−74,77] Assignment of vibrational bands to different ion associates is not straightforward because of several possible structures and different types of coordination (monovs bidentate);[70,73] MD simulations provide therefore valuable information on local structure, supplementing spectroscopic data. Further complications arise from the possibility of different conformations of $TFSI^-$ or FSI^- anions. According to quantum-chemical calculations, *cis* and *trans* conformations of $TFSI^-$ are close in energy[75,78] and its population in real systems is unclear a priori. Spectroscopic data and DFT calculations of ref 77 suggest mixed *cis*/*trans* conformation of $TFSI^-$ interacting with Li^+; on the other hand, preferential *cis* geometry was reported in refs 75 and 78. From the analysis of our results, we have found that the ratio of *cis* and *trans* conformers is about 3:1 in the case of $TFSI^-$ anions; on the other hand, both conformations of FSI^- are approximately equally populated.

Finally, we will turn our attention to the spectroscopic data for ternary electrolytes. Analysis of Raman modes of PEO and $TFSI^-$ anions in ternary electrolyte consisting of poly(ethylene oxide), LiTFSI, and pyrrolidinium-TFSI IL showed that Li^+−PEO and Li^+−$TFSI^-$ interactions compete in ternary mixtures, and both kinds of interactions are reduced in ternary electrolyte compared to corresponding binary systems, suggesting mixed Li^+ coordination.[24] Similar was the effect of functionalizing IL cation with ether side chain: average number of $TFSI^-$ anions in Li^+ solvation shell was reduced from 2.1−2.3 to 1.6−1.9.[29] Such effect of competing Li^+−O_{TFSI} and Li^+−O_{glyme} interactions is visible in our high-temperature results for systems with EMIM-TFSI.

According to the data presented in Figures 6 and 7 and in Table 4, we may distinguish four different types of structures found in our HG/salt/IL systems. The first two are the systems with EMIM-BF_4 and EMIM-PF_6 in which ionic liquid and hexaglyme form two separate phases. In the first system, Li^+ cations are practically exclusively dissolved in the EMIM-BF_4 phase. In the other, they reside at the interface between two liquids; therefore, the lithium cation is coordinated both to fluorine atoms from PF_6^- and to oxygen atoms from hexaglyme molecules. The other types of structures are the systems based on EMIM-TFSI, EMIM-FSI, and EMIM-$B(CN)_4$ in which cases mixing of HG and IL is much better. Phase separation, if present at all, is limited to aggregates of only a few molecules or ions. The difference between these systems is again in the Li^+ coordination. In HG/EMIM-TFSI mixture, lithium cation is approximately equally coordinated to hexaglyme and to $TFSI^-$ anion. Conversely, in HG/EMIM-FSI and HG/EMIM-$B(CN)_4$, the cation interacts mainly with oxygen atoms of hexaglyme, coordination to oxygen atoms from FSI^- is much

DOI: 10.1021/acs.jpcb.5b05705
J. Phys. Chem. B 2015, 119, 11708−11720

smaller, and coordination to tetracyanoborate anions is negligible. Therefore, latter two systems may be viewed as Li^+−hexaglyme complexes dissolved in EMIM-FSI or EMIM-$B(CN)_4$ ionic liquids.

At this point we try to rationalize these results using the binding and the interaction energies calculated in explicit solvent and presented in the preceding section. First, we note that interaction energies of Li^+ or anions with the solvent are more negative in the ionic liquid than in hexaglyme. In the case of anions, the difference between HG and IL does not depend much on the IL: in hexaglyme, E^{int} values for all anions are about −50 kcal/mol, and in ILs, they range from about −70 to −80 kcal/mol.[52] Interaction energy of Li^+ with hexaglyme is −128 kcal/mol, and it is the same as the interaction energy with EMIM-$B(CN)_4$ and only about 10 kcal/mol different from the interaction with EMIM-FSI. However, E^{int} decreases to −156 and −173 kcal/mol in EMIM-PF_6 and EMIM-BF_4, respectively. On the grounds of calculated E^{int}, all ions should tend to be solvated in IL phase (with the exception of EMIM-$B(CN)_4$) because of more stabilizing interaction energies. This should be especially pronounced for Li^+ in ionic liquids based on PF_6^- and BF_4^- anions.

The other clue comes from the binding energies of Li^+−glyme complexes in HG and ILs (Figure 4) which apparently correlate with the type of Li^+ coordination. Binding energies in EMIM-TFSI and EMIM-PF_6 are similar to the values calculated in hexaglyme. Almost all complexes in EMIM-FSI or EMIM-$B(CN)_4$ are more stable than in HG; conversely, binding energies in EMIM-BF_4 are more positive. In particular, this regards all complexes with coordination number equal to 5 and most complexes with CN = 4, i.e., those most relevant to Li^+ coordination in real systems.

Both interaction energies and binding energies are therefore consistent with observed structures of HG/IL mixtures. Solvation of Li^+ in EMIM-BF_4 is highly favorable, but Li^+−glyme complexes are unstable in this IL. As a result, all Li cations reside in IL phase and both liquids separate. Stability of Li^+−glyme aggregates in HG and EMIM-TFSI or EMIM-PF_6 is comparable; accordingly, Li^+ ions locate between these two phases and the cations are coordinated both to IL anions and to HG molecules. Coordination to HG increases in EMIM-TFSI in accord with higher E^{int} values, making solvation of Li^+ in this IL not as much favorable as in EMIM-PF_6. Finally, Li^+ interaction with the solvent is not much different in HG and EMIM-FSI (only 9 kcal/mol difference), and it is the same in HG and EMIM-$B(CN)_4$; therefore, solvation in HG competes with interaction with IL. Moreover, Li^+−glyme binding energies are more stabilizing in EMIM-FSI or EMIM-$B(CN)_4$; therefore, Li^+ ions present in the IL phase are still complexed by HG oxygen atoms. Accordingly, Li^+ cation binds to HG as seen in Table 4, and both HG and IL phases are relatively well mixed.

We may now summarize our explicit solvent calculations for limited system sizes showing differences in interaction and binding energies between ionic liquids depending on their anion. Stabilization of Li^+ ion in ILs with EMIM cation and different anions increases in the sequence $B(CN)_4^- < FSI^- < TFSI^- < PF_6^- < BF_4^-$. Relative stabilities of Li^+−glyme complexes in ionic liquids decrease in the same order. We should note that the correlation between electrolyte structure and binding energies is valid only for explicit solvent model. All five ILs have similar dielectric constant, and the Li^+ interaction energies and binding energies in implicit model are similar in all ILs; thus, the PCM will not differentiate between ionic liquids. The difference is observable in the explicit model treating the solution at molecular level, which is therefore being capable of accounting for specific interactions. On the other hand, the PCM can predict the difference between molecular and ionic liquid, yet the size of the effect is significantly smaller than that resulting from the explicit approach.

Structural features (Li^+−glyme and Li^+−anion distances and the type of Li^+−anion coordination) of electrolytes found in MD simulations agree with available literature data. In simulations we observed different structures of lithium salt in mixed hexaglyme/IL solvent, ranging from rather homogeneous to phase-separated. Depending on the anion of the salt and ionic liquid, studied electrolytes exhibited different coordination of Li^+ cation: from prevailing coordination to oligoether in EMIM-$B(CN)_4$ or EMIM-FSI to dominant interactions with BF_4^- in EMIM-BF_4. Effects of IL addition to oligoglyme/salt electrolyte may be therefore very different for different anions of the IL. Ionic liquids with $B(CN)_4^-$ or FSI^- anions barely affect Li^+−PEO association. EMIM-TFSI or EMIM-PF_6 decrease strength of Li^+−glyme interactions and lead to mixed Li^+ coordination to glyme molecules and to salt/IL anion. Finally, in the systems with EMIM-BF_4, two phases separate and Li^+−glyme association is broken, with metal cations solvated in the IL phase. We were able to relate these structural properties of ternary mixtures to interaction and complexation energies computed within the explicit solvent approach. Effectiveness of an IL in reducing Li^+−PEO interactions apparently correlates with the sequence of anions exhibiting increasing tendency toward aggregation in Li−glyme solvates.[68] Dependence of preferred Li^+ coordination on the type of salt/IL anion and different degree of homogeneity observed in simulations suggest that these properties may be modified by a proper choice of salt and the liquid (including the possibility of using the competition between Li^+ affinity to different anions in systems with different anions of salt and IL). Further studies on electrolytes with other anions could help to verify the correlation mentioned above, which might then serve as a guide for salt selection. Spectroscopic measurements on ternary electrolytes would be desirable to get experimental insight into Li^+ coordination in such systems.

5. CONCLUSIONS

We used molecular dynamics simulations combined with calculations of binding energies to study model ternary electrolytes based on PEO, lithium salts, and five EMIM-based ionic liquids. We compared predictions of explicit and continuous solvent models and have related them to the structures observed in MD trajectories.

Our results of explicit solvent modeling suggest that for molecular solvents estimates of interaction and binding energies in solution may be obtained for about explicit 20 solvent molecules. Conversely, long-range structure of solvation shells for charged solutes in ionic liquids increases the size of the system needed to converge results, making investigations of solvent effects in explicit ILs a challenging task.

Results of this work led to the conclusion that in complex systems with ionic liquids, implicit solvent models are prone to fail because they rely to a large extent on macroscopic dielectric permittivity of the solvent, applicability of which to the description of ILs is questionable.[87] In particular, continuous models may be incapable of proper reproduction of differences between liquids. The explicit solvent approach seems much more promising in this context; however, it requires usually

DOI: 10.1021/acs.jpcb.5b05705
J. Phys. Chem. B 2015, 119, 11708−11720

molecular dynamics stage for structure generation, and the cost of quantum-chemical calculations for relevant system sizes is prohibitive. Therefore, force-field-based methods including energy calculations and classical molecular dynamics simulations may be indispensable in the modeling of multicomponent solvent systems.

■ ASSOCIATED CONTENT

Supporting Information

The Supporting Information is available free of charge on the ACS Publications website at DOI: 10.1021/acs.jpcb.5b05705.

Structures of Li^+−glyme complexes, comparison of force field and QC calculations, RDFs for EMIM-$B(CN)_4$ and for low temperature, estimates of diffusion coefficients and conductivity (PDF)

■ AUTHOR INFORMATION

Corresponding Author

*Fax: +48 12 6340515. E-mail: eilmes@chemia.uj.edu.pl.

Notes

The authors declare no competing financial interest.

■ ACKNOWLEDGMENTS

This work was supported by the National Science Centre (Poland) Grant 2012/07/B/ST4/00573. The research was supported by PL-Grid computational infrastructure. Part of the equipment used in calculations was purchased with the financial support from the European Regional Development Fund in the framework of the Polish Innovation Economy Operational Program (Contract POIG.02.01.00-12-023/08).

■ REFERENCES

(1) Meyer, W. H. Polymer Electrolytes for Lithium-Ion Batteries. *Adv. Mater.* **1998**, *10*, 439−448.

(2) Dias, F. B.; Plomp, L.; Veldhuis, J. B. J. Trends in Polymer Electrolytes for Secondary Lithium Batteries. *J. Power Sources* **2000**, *88*, 169−191.

(3) Agrawal, R. C.; Pandey, G. P. Solid Polymer Electrolytes: Materials Designing and All-Solid-State Battery Applications: An Overview. *J. Phys. D: Appl. Phys.* **2008**, *41*, 223001.

(4) Marcinek, M.; Syzdek, J.; Marczewski, M.; Piszcz, M.; Niedzicki, L.; Kalita, M.; Plewa-Marczewska, A.; Bitner, A.; Wieczorek, P.; Trzeciak, T.; Kasprzyk, M.; Łężak, P.; Zukowska, Z.; Zalewska, A.; Wieczorek, W. Electrolytes for Li-Ion Transport − Review. *Solid State Ionics* **2015**, *276*, 107−126.

(5) Fenton, D. E.; Parker, J. M.; Wright, P. V. Complexes of Alkali Metal Ions with Poly(ethylene oxide). *Polymer* **1973**, *14*, 589.

(6) Müller-Plathe, F.; van Gustersen, W. F. Computer Simulation of a Polymer Electrolyte: Lithium Iodide in Amorphous Poly(ethylene oxide). *J. Chem. Phys.* **1995**, *103*, 4745−4756.

(7) Berthier, C.; Górecki, W.; Minier, M.; Armand, M. B.; Chabagno, B.; Rigaud, P. Microscopic Investigation of Ionic-Conductivity in Alkali-Metal Salts Poly(ethylene oxide) Adducts. *Solid State Ionics* **1983**, *11*, 91−95.

(8) Song, J. Y.; Wang, Y. Y.; Wan, C. C. Review of Gel-Type Polymer Electrolytes for Lithium-Ion Batteries. *J. Power Sources* **1999**, *77*, 183−197.

(9) Stephan, A. M. Review on Gel Polymer Electrolytes for Lithium Batteries. *Eur. Polym. J.* **2006**, *42*, 21−42.

(10) Hallett, J. P.; Welton, T. Room-Temperature Ionic Liquids: Solvents for Synthesis and Catalysis. 2. *Chem. Rev.* **2011**, *111*, 3508−3576.

(11) Zhang, S.; Sun, J.; Zhang, X.; Xin, J.; Miao, Q.; Wang, J. Ionic Liquid-Based Green Processes for Energy Production. *Chem. Soc. Rev.* **2014**, *43*, 7838−7869.

(12) Diddens, D.; Heuer, A. Simulation Study of the Lithium Ion Transport Mechanism in Ternary Polymer Electrolytes: The Critical Role of the Segmental Mobility. *J. Phys. Chem. B* **2014**, *118*, 1113−1125.

(13) Egashira, M.; Todo, H.; Yoshimoto, N.; Morita, M. Lithium Ion Conduction in Ionic Liquid-Based Gel Polymer Electrolyte. *J. Power Sources* **2008**, *178*, 729−735.

(14) Abitelli, A.; Ferrari, S.; Quartarone, E.; Mustarelli, P.; Magistris, A.; Fagnoni, M.; Albini, A.; Gerbaldi, C. Polyethylene Oxide Electrolyte Membranes with Pyrrolidinium-Based Ionic Liquids. *Electrochim. Acta* **2010**, *55*, 5478−5484.

(15) Kim, G. T.; Appetecchi, G. B.; Carewska, M.; Joost, M.; Balducci, A.; Winter, M.; Passerini, S. UV Cross-Linked, Lithium-Conducting Ternary Polymer Electrolytes Containing Ionic Liquids. *J. Power Sources* **2010**, *195*, 6130−6137.

(16) Bayley, P. M.; Lane, G. H.; Lyons, L. J.; MacFarlane, D. R.; Forsyth, M. Undoing Lithium Ion Association in Ionic Liquids through the Complexation by Oligoethers. *J. Phys. Chem. C* **2010**, *114*, 20569−20576.

(17) Kumar, Y.; Hashmi, S. A.; Pandey, G. P. Ionic Liquid Mediated Magnesium Ion Conduction in Poly(ethylene oxide) Based Polymer Electrolyte. *Electrochim. Acta* **2011**, *56*, 3864−3873.

(18) Desai, S.; Shepherd, R. L.; Innis, P. C.; Murphy, P.; Hall, C.; Fabretto, R.; Wallace, G. G. Gel Electrolytes with Ionic Liquid Plasticiser for Electrochromic Devices. *Electrochim. Acta* **2011**, *56*, 4408−4413.

(19) Egashira, M.; Asai, M.; Yoshimoto, N.; Morita, M. Ionic Conductivity of Ternary Electrolyte Containing Sodium Salt and Ionic Liquid. *Electrochim. Acta* **2011**, *58*, 95−98.

(20) Pandey, G. P.; Kumar, Y.; Hashmi, S. A. Ionic Liquid Incorporated PEO Based Polymer Electrolyte for Electrical Double Layer Capacitors: A Comparative Study with Lithium and Magnesium Systems. *Solid State Ionics* **2011**, *190*, 93−98.

(21) Kumar, Y.; Hashmi, S. A.; Pandey, G. P. Lithium Ion Transport and Ion−Polymer Interaction in PEO Based Polymer Electrolyte Plasticized with Ionic Liquid. *Solid State Ionics* **2011**, *201*, 73−80.

(22) Chaurasia, S. K.; Singh, R. K.; Chandra, S. Ion−Polymer and Ion−Ion Interaction in PEO-Based Polymer Electrolytes Having Complexing Salt $LiClO_4$ and/or Ionic Liquid, [BMIM][PF_6]. *J. Raman Spectrosc.* **2011**, *42*, 2168−2172.

(23) Wang, H.; Imanishi, N.; Hirano, A.; Takeda, Y.; Yamamoto, O. Electrochemical Properties of the Polyethylene Oxide-Li$(CF_3SO_2)_2N$ and Ionic Liquid Composite Electrolyte. *J. Power Sources* **2012**, *219*, 22−28.

(24) Joost, M.; Kunze, M.; Jeong, S.; Schönhoff, M.; Winter, M.; Passerini, S. Ionic Mobility in Ternary Polymer Electrolytes for Lithium-Ion Batteries. *Electrochim. Acta* **2012**, *86*, 330−338.

(25) Wetjen, M.; Kim, G.-T.; Joost, M.; Winter, M.; Passerini, S. Temperature Dependence of Electrochemical Properties of Cross-Linked Poly(ethylene oxide)−Lithium Bis(trifluoromethanesulfonyl)-imide−N-butyl-N-methylpyrrolidinium Bis(trifluoromethanesulfonyl)-imide Solid Polymer Electrolytes for Lithium Batteries. *Electrochim. Acta* **2013**, *87*, 779−787.

(26) Rajput, D. S.; Yamada, K.; Sekhon, S. S. Study of Ion Diffusional Motion in Ionic Liquid-Based Polymer Electrolytes by Simultaneous Solid State NMR and DTA. *J. Phys. Chem. B* **2013**, *117*, 2475−2481.

(27) Kösters, J.; Schönhoff, M.; Stolwijk, N. A. Ion Transport Effects in a Solid Polymer Electrolyte Due to Salt Substitution and Addition Using an Ionic Liquid. *J. Phys. Chem. B* **2013**, *117*, 2527−2534.

(28) Monteiro, M. J.; Camilo, F. F.; Ribeiro, M. C. C.; Torresi, R. M. Ether-Bond-Containing Ionic Liquids and the Relevance of the Ether Bond Position to Transport Properties. *J. Phys. Chem. B* **2010**, *114*, 12488−12494.

(29) Kunze, M.; Paillard, E.; Jeong, S.; Appetecchi, G. B.; Schönhoff, M.; Winter, M.; Passerini, S. Inhibition of Self-Aggregation in Ionic Liquid Electrolytes for High-Energy Electrochemical Devices. *J. Phys. Chem. C* **2011**, *115*, 19431−19436.

DOI: 10.1021/acs.jpcb.5b05705
J. Phys. Chem. B 2015, 119, 11708−11720

(30) Rennie, A. J. R.; Sanchez-Ramirez, N.; Torresi, R. M.; Hall, P. J. Ether-Bond-Containing Ionic Liquids as Supercapacitor Electrolytes. *J. Phys. Chem. Lett.* **2013**, *4*, 2970−2974.
(31) Costa, L. T.; Ribeiro, M. C. C. Molecular Dynamics Simulation of Polymer Electrolytes Based on Poly(ethylene oxide) and Ionic Liquids. I. Structural Properties. *J. Chem. Phys.* **2006**, *124*, 184902.
(32) Costa, L. T.; Ribeiro, M. C. C. Molecular Dynamics Simulation of Polymer Electrolytes Based on Poly(ethylene oxide) and Ionic Liquids. II. Dynamical Properties. *J. Chem. Phys.* **2007**, *127*, 164901.
(33) Figueiredo, P. H.; Siqueira, L. J. A.; Ribeiro, M. C. C. The Equilibrium Structure of Lithium Salt Solutions in Ether-Functionalized Ammonium Ionic Liquids. *J. Phys. Chem. B* **2012**, *116*, 12319−12324.
(34) Chattoraj, J.; Diddens, D.; Heuer, A. Effects of Ionic Liquids on Cation Dynamics in Amorphous Polyethylene Oxide Electrolytes. *J. Chem. Phys.* **2014**, *140*, 024906.
(35) Gejji, S. P.; Johansson, P.; Tegenfeldt, J.; Lindgren, J. Conformational Changes Induced by Metal-Ion Coordination - Lithium(I)-Diglyme. *Comput. Polym. Science* **1995**, *5*, 99−105.
(36) Sutjianto, A.; Curtiss, L. A. Li^+ -Diglyme Complexes: Barriers to Lithium Cation Migration. *J. Phys. Chem. A* **1998**, *102*, 968−974.
(37) Johansson, P.; Tegenfeldt, J.; Lindgren, J. Modelling Amorphous Lithium Salt−PEO Polymer Electrolytes: Ab Initio Calculations of Lithium Ion−Tetra-, Penta- and Hexaglyme Complexes. *Polymer* **1999**, *40*, 4399−4406.
(38) Baboul, A. G.; Redfern, P. C.; Sutjianto, A.; Curtiss, L. A. Li^+ -$(Diglyme)_2$ and $LiClO_4$ -Diglyme Complexes: Barriers to Lithium Ion Migration. *J. Am. Chem. Soc.* **1999**, *121*, 7220−7227.
(39) Redfern, P. C.; Curtiss, L. A. Quantum Chemical Studies of Li^+ Cation Binding to Polyalkyloxides. *J. Power Sources* **2002**, *110*, 401−405.
(40) Kirchner, B. Ionic Liquids from Theoretical Investigations. *Top. Curr. Chem.* **2008**, *290*, 213−262.
(41) Bodo, E.; Caminiti, R. The Structure of Geminal Imidazolium Bis(trifluoromethylsulfonyl)amide Ionic Liquids: A Theoretical Study of the Gas Phase Ionic Complexes. *J. Phys. Chem. A* **2010**, *114*, 12506−12512.
(42) Angenendt, K.; Johansson, P. Ionic Liquid Structures from Large Density Functional Theory Calculations Using Mindless Configurations. *J. Phys. Chem. C* **2010**, *114*, 20577−20582.
(43) Fernandes, A. M.; Rocha, M. A. A.; Freire, M. G.; Marrucho, I. M.; Coutinho, J. A. P.; Santos, L. M. N. B. F. Evaluation of Cation-Anion Interaction Strength in Ionic Liquids. *J. Phys. Chem. B* **2011**, *115*, 4033−4041.
(44) Zahn, S.; MacFarlane, D. R.; Izgorodina, W. I. Assessment of Kohn−Sham Density Functional Theory and Møller−Plesset Perturbation Theory for Ionic Liquids. *Phys. Chem. Chem. Phys.* **2013**, *15*, 13664−13675.
(45) Klamt, A.; Schüürmann, G. COSMO - a New Approach to Dielectric Screening in Solvents with Explicit Expressions for the Screening Energy and its Gradient. *J. Chem. Soc., Perkin Trans. 2* **1993**, *5*, 799−805.
(46) Miertuš, S.; Scrocco, E.; Tomasi, J. Electrostatic Interaction of a Solute with a Continuum - A Direct Utilization of Ab Initio Molecular Potentials for the Prevision of Solvent Effects. *Chem. Phys.* **1981**, *55*, 117−129.
(47) Johansson, P.; Jacobsson, P. Lithium Salt Dissociation in Non-Aqueous Electrolytes Modeled by Ab Initio Calculations. *Solid State Ionics* **2006**, *177*, 2691−2697.
(48) Johansson, P. Electronic Structure Calculations on Lithium Battery Electrolyte Salts. *Phys. Chem. Chem. Phys.* **2007**, *9*, 1493−1498.
(49) Eilmes, A.; Kubisiak, P. Polarizable Continuum Model Study on the Solvent Effect of Polymer Matrix in Poly(ethylene oxide)-Based Solid Electrolyte. *J. Phys. Chem. A* **2008**, *112*, 8849−8857.
(50) Eilmes, A.; Kubisiak, P. A Quantum-Chemical Study on the Boron Centers in Nonaqueous Electrolyte Solutions and Polymer Electrolytes. *Electrochim. Acta* **2011**, *56*, 3219−3224.
(51) Borodin, O. Polarizable Force Field Development and Molecular Dynamics Simulations of Ionic Liquids. *J. Phys. Chem. B* **2009**, *113*, 11463−11478.
(52) Eilmes, A.; Kubisiak, P. Stability of Ion Triplets in Ionic Liquid/Lithium Salt Solutions: Insights from Implicit and Explicit Solvent Models and Molecular Dynamics Simulations. *J. Comput. Chem.* **2015**, *36*, 751−762.
(53) Eilmes, A.; Kubisiak, P. Molecular Dynamics Study on the Effect of Lewis Acid Centers in Poly(ethylene oxide)/$LiClO_4$ Polymer Electrolyte. *J. Phys. Chem. B* **2011**, *115*, 14938−14946.
(54) Martínez, L.; Andrade, R.; Birgin, E. G.; Martínez, J. M. Packmol: A Package for Building Initial Configurations for Molecular Dynamics Simulations. *J. Comput. Chem.* **2009**, *30*, 2157−2164.
(55) Tinker Molecular Modeling Package, v. 5.1. http://dasher.wustl.edu/tinker/.
(56) Berendsen, H. J. C.; Postma, J. P. M.; van Gunstersen, W. F.; DiNola, A.; Haak, J. R. Molecular Dynamics with Coupling to an External Bath. *J. Chem. Phys.* **1984**, *81*, 3684−3690.
(57) Beeman, D. Some Multistep Methods for Use in Molecular Dynamics Calculations. *J. Comput. Phys.* **1976**, *20*, 130−139.
(58) Toukmaji, A. Y.; Board, J. A., Jr. Ewald Summation Techniques in Perspective: A Survey. *Comput. Phys. Commun.* **1996**, *95*, 73−92.
(59) Thole, B. T. Molecular Polarizabilities Calculated with a Modified Dipole Interaction. *Chem. Phys.* **1981**, *59*, 341−350.
(60) Eilmes, A.; Sterzel, M.; Szepieniec, T.; Kocot, J.; Noga, K.; Golik, M. Comprehensive Support for Chemistry Computations in PL-Grid Infrastructure. In *eScience on Distributed Computing Infrastructure: Lecture Notes in Computer Science*; Bubak, M., Kitowski, J., Wiatr, K., Eds.; Springer International Publishing, Switzerland, 2014; Vol. *8500*, pp 250−263.
(61) Frisch, M. J.; Trucks, G. W.; Schlegel, H. B.; Scuseria, G. E.; Robb, M. A.; Cheeseman, J. R.; Scalmani, G.; Barone, V.; Mennucci, B.; Petersson, G. A.; Nakatsuji, H.; Caricato, M.; Li, X.; Hratchian, H. P.; Izmaylov, A. F.; Bloino, J.; Zheng, G.; Sonnenberg, J. L.; Hada, M.; Ehara, M.; Toyota, K.; Fukuda, R.; Hasegawa, J.; Ishida, M.; Nakajima, T.; Honda, Y.; Kitao, O.; Nakai, H.; Vreven, T.; Montgomery, Jr., J. A.; Peralta, J. E.; Ogliaro, F.; Bearpark, M.; Heyd, J. J.; Brothers, E.; Kudin, K. N.; Staroverov, V. N.; Kobayashi, R.; Normand, J.; Raghavachari, K.; Rendell, A.; Burant, J. C.; Iyengar, S. S.; Tomasi, J.; Cossi, M.; Rega, N.; Millam, J. M.; Klene, M.; Knox, J. E.; Cross, J. B.; Bakken, V.; Adamo, C.; Jaramillo, J.; Gomperts, R.; Stratmann, R. E.; Yazyev, O.; Austin, A. J.; Cammi, R.; Pomelli, C.; Ochterski, J. W.; Martin, R. L.; Morokuma, K.; Zakrzewski, V. G.; Voth, G. A.; Salvador, P.; Dannenberg, J. J.; Dapprich, S.; Daniels, A. D.; Farkas, Ö.; Foresman, J. B.; Ortiz, J. V.; Cioslowski, J.; Fox, D. J. *Gaussian 09*, revision D.01; Gaussian, Inc.: Wallingford CT, 2009.
(62) TeraChem, v. 1.5. PetaChem, LLC. http://www.petachem.com/.
(63) Grimme, S.; Antony, J.; Ehrlich, S.; Krieg, H. A Consistent and Accurate Ab Initio Parametrization of Density Functional Dispersion Correction (DFT-D) for the 94 Elements H-Pu. *J. Chem. Phys.* **2010**, *132*, 154104.
(64) Marenich, A. V.; Cramer, C. J.; Truhlar, D. G. Universal Solvation Model Based on Solute Electron Density and on a Continuum Model of the Solvent Defined by the Bulk Dielectric Constant and Atomic Surface Tensions. *J. Phys. Chem. B* **2009**, *113*, 6378−6396.
(65) Henderson, W. A.; Brooks, N. R.; Brennessel, W. W.; Young, V. G. Triglyme-Li^+ Cation Solvate Structures: Models for Amorphous Concentrated Liquid and Polymer Electrolytes (I). *Chem. Mater.* **2003**, *15*, 4679−4684.
(66) Henderson, W. A.; Brooks, N. R.; Young, V. G. Tetraglyme-Li^+ Cation Solvate Structures: Models for Amorphous Concentrated Liquid and Polymer Electrolytes (II). *Chem. Mater.* **2003**, *15*, 4685−4690.
(67) Henderson, W. A.; McKenna, F.; Khan, M. A.; Brooks, N. R.; Young, V. G.; Frech, R. Glyme-Lithium Bis(trifluoromethanesulfonyl)-imide and Glyme-Lithium Bis(perfluoroethanesulfonyl)imide Phase Behavior and Solvate Structures. *Chem. Mater.* **2005**, *17*, 2284−2289.

DOI: 10.1021/acs.jpcb.5b05705
J. Phys. Chem. B 2015, 119, 11708−11720

(68) Henderson, W. A. Glyme-Lithium Salt Phase Behavior. *J. Phys. Chem. B* **2006**, *110*, 13177−13183.
(69) Zhang, C.; Ueno, K.; Yamazaki, A.; Yoshida, K.; Moon, H.; Mandai, T.; Umebayashi, Y.; Dokko, K.; Watanabe, M. Chelate Effects in Glyme/Lithium Bis(trifluoromethanesulfonyl)amide Solvate Ionic Liquids. I. Stability of Solvate Cations and Correlation with Electrolyte Properties. *J. Phys. Chem. B* **2014**, *118*, 5144−5133.
(70) Seo, D. M.; Boyle, P. D.; Sommer, R. D.; Daubert, J. S.; Borodin, O.; Henderson, W. A. Solvate Structures and Spectroscopic Characterization of LiTFSI Electrolytes. *J. Phys. Chem. B* **2014**, *118*, 13601−13608.
(71) Zhang, C.; Yamazaki, A.; Murai, J.; Park, J.-W.; Mandai, T.; Ueno, K.; Dokko, K.; Watanabe, M. Chelate Effects in Glyme/Lithium Bis(trifluoromethanesulfonyl)amide Solvate Ionic Liquids, Part 2: Importance of Solvate-Structure Stability for Electrolytes of Lithium Batteries. *J. Phys. Chem. C* **2014**, *118*, 17362−17373.
(72) Seo, D. M.; Boyle, P. D.; Allen, J. L.; Han, S.-D.; Jónsson, E.; Johansson, P.; Henderson, W. A. Solvate Structures and Computational/Spectroscopic Characterization of $LiBF_4$ Electrolytes. *J. Phys. Chem. C* **2014**, *118*, 18377−18386.
(73) Han, S.-D.; Yun, S.-H.; Borodin, O.; Seo, D. M.; Sommer, R. D.; Young, V. G., Jr.; Henderson, W. A. Solvate Structures and Computational/Spectroscopic Characterization of $LiPF_6$ Electrolytes. *J. Phys. Chem. C* **2015**, *119*, 8492−8500.
(74) Ueno, K.; Tatara, R.; Tsuzuki, S.; Saito, S.; Doi, H.; Yoshida, K.; Mandai, T.; Matsugami, M.; Umebayashi, Y.; Dokko, K.; Watanabe, M. Li^+ Solvation in Glyme−Li Salt Solvate Ionic Liquids. *Phys. Chem. Chem. Phys.* **2015**, *17*, 8248−8257.
(75) Umebayashi, U.; Mitsugi, T.; Fukuda, S.; Fujimori, T.; Fujii, K.; Kanzaki, R.; Takeuchi, M.; Ishiguro, S. Lithium Ion Solvation in Room-Temperature Ionic Liquids Involving Bis-(trifluoromethanesulfonyl) Imide Anion Studied by Raman Spectroscopy and DFT Calculations. *J. Phys. Chem. B* **2007**, *111*, 13028−13032.
(76) Monteiro, M. J.; Bazito, F. F. C.; Siqueira, L. J. A.; Ribeiro, M. C. C.; Torresi, R. M. Transport Coefficients, Raman Spectroscopy, and Computer Simulation of Lithium Salt Solutions in an Ionic Liquid. *J. Phys. Chem. B* **2008**, *112*, 2102−2109.
(77) Lassègues, J.-C.; Grondin, J.; Aupetit, Ch.; Johansson, P. Spectroscopic Identification of the Lithium Ion Transporting Species in LiTFSI-Doped Ionic Liquids. *J. Phys. Chem. A* **2009**, *113*, 305−314.
(78) Umebayashi, Y.; Mori, S.; Fujii, K.; Tsuzuki, S.; Seki, S.; Hayamizu, K.; Ishiguro, S. Raman Spectroscopic Studies and Ab Initio Calculations on Conformational Isomerism of 1-Butyl-3-methylimidazolium Bis-(trifluoromethanesulfonyl)amide Solvated to a Lithium Ion in Ionic Liquids: Effects of the Second Solvation Sphere of the Lithium Ion. *J. Phys. Chem. B* **2010**, *114*, 6513−6521.
(79) Scheers, J.; Pitawala, J.; Thebault, F.; Kim, J.-K.; Ahn, J.-H.; Matic, A.; Johansson, P.; Jacobsson, P. Ionic Liquids and Oligomer Electrolytes Based on the $B(CN)_4^-$ Anion; Ion Association, Physical and Electrochemical Properties. *Phys. Chem. Chem. Phys.* **2011**, *13*, 14953−14959.
(80) Yu, L.; Pizio, B. S.; Vaden, T. D. Conductivity and Spectroscopic Investigation of Bis(trifluoromethanesulfonyl)imide Solution in Ionic Liquid 1-Butyl-3-methylimidazolium Bis(trifluoromethanesulfonyl)-imide. *J. Phys. Chem. B* **2012**, *116*, 6553−6560.
(81) Fujii, K.; Hamano, H.; Doi, H.; Song, X.; Tsuzuki, S.; Hayamizu, K.; Seki, S.; Kameda, Y.; Dokko, K.; Watanabe, M.; Umebayashi, Y. Unusual Li^+ Ion Solvation Structure in Bis(fluorosulfonyl)amide Based Ionic Liquid. *J. Phys. Chem. C* **2013**, *117*, 19314−19324.
(82) Solano, C. J. F.; Jeremias, S.; Paillard, E.; Beljonne, D.; Lazzaroni, R. A Joint Theoretical/Experimental Study of the Structure, Dynamics, and Li^+ Transport in Bis([tri]fluoro[methane]sulfonyl)-imide [T]FSI-Based Ionic Liquids. *J. Chem. Phys.* **2013**, *139*, 034502.
(83) Haskins, J. B.; Bennett, W. R.; Wu, J. L.; Hernández, D. M.; Borodin, O.; Monk, J. D.; Bauschlicher, C. W., Jr.; Lawson, J. W. Computational and Experimental Investigation of Li-Doped Ionic Liquid Electrolytes: [pyr14][TFSI], [pyr13][FSI], and $[EMIM][BF_4]$. *J. Phys. Chem. B* **2014**, *118*, 11295−11309.
(84) Borodin, O.; Smith, G. D.; Douglas, R. Force Field Development and MD Simulations of Poly(ethylene oxide)/$LiBF_4$ Polymer Electrolytes. *J. Phys. Chem. B* **2003**, *107*, 6824−6837.
(85) Siqueira, L. J. A.; Ribeiro, M. C. C. Molecular Dynamics Simulation of the Polymer Electrolyte Poly(ethylene oxide)/$LiClO_4$. I. Structural Properties. *J. Chem. Phys.* **2005**, *122*, 194911.
(86) Borodin, O.; Smith, G. D. Mechanism of Ion Transport in Amorphous Poly(ethylene oxide)/LiTFSI from Molecular Dynamics Simulations. *Macromolecules* **2006**, *39*, 1620−1629.
(87) Kobrak, M. N.; Li, H. Electrostatic Interactions in Ionic Liquids: the Dangers of Dipole and Dielectric Descriptions. *Phys. Chem. Chem. Phys.* **2010**, *12*, 1922−1932.

DOI: 10.1021/acs.jpcb.5b05705
J. Phys. Chem. B 2015, 119, 11708−11720